Magnetoreception of photoactivated cryptochrome 1 in electrochemistry and electron transfer

By: Zheng Zeng, Jianjun Wei, Yiyang Liu, Wendi Zhang, and Taylor Mabe

Z. Zeng, J. Wei, Y. Liu, W. Zhang, T. Mabe, Magnetoreception of photoactivated cryptochrome 1 in electrochemistry and electron transfer, *ACS Omega*, **2018**, 3 (5), 4752-4759, DOI: 10.1021/acsomega.8b00645.

Abstract:

Cryptochromes are flavoproteins whose photochemistry is important for crucial functions associated with phototropism and circadian clocks. In this report, we, for the first time, observed a magnetic response of the cryptochrome 1 (CRY1) immobilized at a gold electrode with illumination of blue light. These results present the magnetic field-enhanced photoinduced electron transfer of CRY1 to the electrode by voltammetry, exhibiting magnetic responsive rate constant and electrical current changes. A mechanism of the electron transfer, which involves photoinduced radicals in the CRY, is sensitive to the weak magnetic field; and the long-lived free radical $FAD^{\bullet-}$ is responsible for the detected electrochemical Faradaic current. As a photoreceptor, the finding of a 5.7% rate constant change in electron transfer corresponding to a 50 μT magnetic field may be meaningful in regulation of magnetic field signaling and circadian clock function under an electromagnetic field.

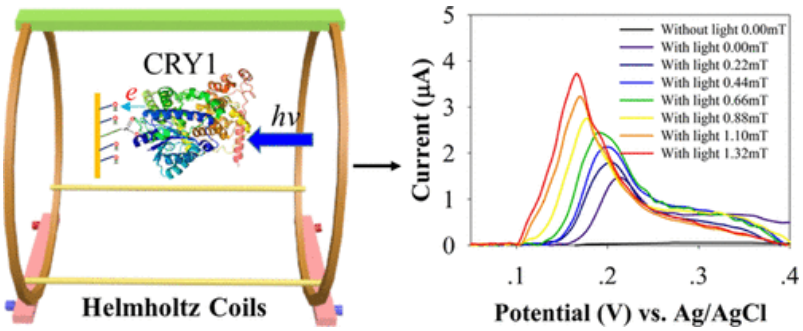

Keywords: cryptochrome 1 (CRY1) | magnetic response | tryptophan

Article:

Introduction

Cryptochromes (CRYs) are a class of flavoproteins as photoreceptors with the cryptic nature for a long time.(1) A CRY, as a photoactive pigment, was first discovered in *Arabidopsis thaliana*(2) and *Sinapis alba*(3) and has high sequence homology to photolyase.(4) CRYs have no photolyase

activity for DNA repair,[5] though CRYs and photolyases belong to the same family of flavoproteins with high sequence identity.[5−7] Later, they were also identified to function as blue-light photoreceptors in insects for synchronizing the circadian clock.[8−10]

CRYs and photolyases have similar three-dimensional structures.[11] Most CRYs, like all the flavoproteins superfamily, are composed of two domains, an amino (N)-terminal photolyase-related (PHR) region and a carboxy (C)-terminal domain of varying sizes.[12] The N-terminal PHR domain can noncovalently bind to a single molecule of the flavin adenine dinucleotide (FAD) cofactor and a light-harvesting chromophore.[13] The second chromophore can be either pterin or deazaflavin.[5,14] The C-terminal domain is less conserved than the PHR domain. The structure of the CRY1 protein is primarily made up of alpha helices with a few loops and beta sheets. The PHR region has two domains, the α/β domain and a helical domain, which are connected by a variable loop that wraps around the α/β domain. The α/β domain adopts a dinucleotide-binding fold with five-strand parallel β sheets flanked on either side by α helices. Two lobes of the helical domain form a cavity called the FAD-access cavity.[12] FAD is buried deeply inside the FAD-access cavity, but it may be accessible to the solvent from the bottom of the cavity. FAD noncovalently binds to the protein in a U-shaped conformation, with its adenine and isoalloxazine rings positioned at the bottom of the cavity. Different from photolyase, which is generally positively charged, the surface of CRY1 PHR is predominantly negatively charged, except for a small concentration of positive charges near the FAD-access cavity.[13]

CRYs, as blue light photoreceptors, have a variety of known functions including phototropism, circadian rhythms, and light-dependent regulation of plant growth and development.[15] CRYs have also been proposed as candidate magnetoreceptors.[16] Over half a century, many researchers have reported that plants[17−19] and animals[20−22] (insects, sea turtles, spotted newts, lobsters, honeybees, European robins, etc.) have the ability to perceive magnetic fields to direct their biological clock, circadian rhythms, and orientation behaviors because of the photoactive magnetoreception role of CRYs. However, the biophysical and chemical basis of the magnetic sense remains elusive.

Magnetoreception of CRYs has been explained by a radical-pair-based mechanism.[16,23] The magnetic sensitivity arises from chemical intermediates formed by photoexcitation of cryptochrome proteins.[24,25] Although the light-induced photocycle in cryptochromes and magnetic field effects in active states of cryptochromes have been examined through transient absorption and electron-spin-resonance observations together with the concept and methods of quantum physics and molecular dynamics,[26−29] the magnetic field-associated electron transfer is less explored.[30,31] More recently, theoretical and spectroscopic studies[32−35] suggest that electron transfer between light-activated FAD and tryptophan (Trp) residues leads to the formation of a spin-correlated radical pair, whose subsequent chemical reactions are sensitive to external magnetic fields. This is because hyperfine coupling (HFC) interactions between an electron spin and a nuclear spin cause the interconversion between the singlet and triplet states of the radical pair, and its dynamics is modulated by an external weak magnetic field. Anisotropies of HFC play a key role in sensing the direction of the magnetic field. In more detail, when a cryptochrome is activated with light, the interconversion of radical pairs of singlet $^{1}[FAD^{\bullet-}\ TrpH^{\bullet+}]$ and triplet $^{3}[FAD^{\bullet-}\ TrpH^{\bullet+}]$ states is critical in determining the response to an external magnetic field.[25] The $^{1}[FAD^{\bullet-}\ TrpH^{\bullet+}]$ can either return to the ground state FAD and

TrpH, or singlet and triplet radical pairs can interconvert and react to generate radicals with uncorrelated electron spins. The fraction of remaining radical pairs and the yield of free radicals depend on the direction/strength of the external magnetic field. This explains the origin of the magnetic field effect. To get a sufficient amount of free radicals, the spin coherence of radical pairs should persist for at least the Larmor period (700 ns for a 50 μT field, the strength for earth's magnetic field).[36] While the oscillations in the spin state of a radical pair are crucial for sensing the existence of an external magnetic field, the product of free radicals stores the magnetic information regarding the magnetic field (e.g., direction and strength) once all radical pairs have disappeared.[25] However, how the protein proceeds to signal the stored information is an unrevealed mystery.

To date, the heterogeneous electron transfer of cryptochromes has not been reported. This is especially true for the magnetic sensitivity of CRYs at a solid interface, which would be of great interest for exploring the associated protein signaling of magnetic information stored in the long-lived free radicals, that is, $FAD^{\bullet-}$ and $TrpH^{\bullet+}$. The free radicals have been proven to return to their resting states by independent redox reactions,[34,37,38] which can potentially be probed by electrochemical means. In addition, the mechanistic structure–function relationship of the CRYs regarding the electron transfer might be examined in a similar way. The hypothesis is that if the electron transfer of the free radicals can be probed with an electrode and examined with respect to an external magnetic field, it could provide an alternative way to investigate and regulate the aspects of magnetic sensing and signaling of the protein.

Cryptochromes play a role in entraining the circadian clock to its environment, circadian photoreceptor,[39,40] and the magnetoreception when excited to form the radical pair.[41] Here, we, for the first time, report magnetic responses by a cyclic voltammetry analysis of the magnetic field effect on the light-induced electron transfer of immobilized cryptochrome 1 (photolyase-like CRY1, MW of 66.2 kDa, Figure S1) on a gold slide. The CRY1 can absorb light at wavelengths ranging from 280 to 500 nm (Figure S2), suggesting its FAD photoreception.[42] The CRY1 is immobilized with a self-assembled monolayer (SAM) of mixed $-S-(CH_2)_{10}-COOH$ and $-S-(CH_2)_8-OH$.[43] The photoactivated CRY1s at the electrode show a strong response in Faradaic current of cyclic voltammetry and the calculated heterogeneous electron transfer rate constant, even to weak external magnetic field flux intensities (0–1.32 mT).

Results and Discussion

Immobilization of CRY1. The surface amino residues at the N-terminal PHR domain favor the cross-link reaction with the activated −COOH, which may enable oriented immobilization of CYR1, at least to some extent (Figure 1). The covalent bonds anchoring the protein should eliminate a gating mechanism for electron transfer of the protein at the surface, resulting from a large conformational motion.[44] While the radical pair model suggests that the proteins would have to be both immobilized and aligned to show anisotropic magnetic responses, the requirement of mutual alignment may not be very strict.[16,45,46] In addition, a small concentration of positive charges near the FAD-access cavity[13] may help to stabilize the conformation of the protein at the gold surface and limit the molecular motion due to the electrostatic force with the negatively charged SAM, making the electron exchange between the FAD complex and a gold electrode possible.

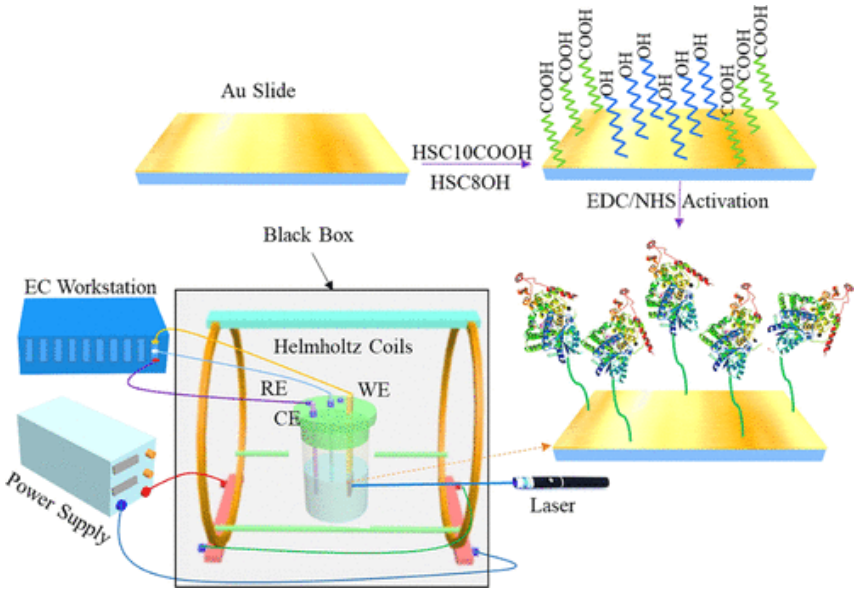

Figure 1. Illustration of the protocol for the SAM formation and CRY1s immobilization on the gold slide electrode and a schematic of the home-setup, optomagnetic electrochemical system used for the electrochemical study of the immobilized CRY1s with a blue light illumination.

Cyclic Voltammetry of Immobilized CRY1s. The stabilized CRY1–SAM–gold electrode was used for the electrochemical testing with respect to the magnetic field and light illumination. Figure 2A shows representative oxidation voltammograms (baseline subtracted from original cyclic voltammograms in Figure S3) of adsorbed CRY1 films with and without blue light excitation at a scan rate of 4 V s^{-1}. CRY1 is known to be activated by light, and no Faradaic signal was observed in the absence of blue light illumination. Upon illumination with blue light, an oxidation peak was observed from the CRY1–SAM–gold electrode. The peak current increased monotonically with increasing magnetic field strength. There is no measurable Faradaic current from the CRY1s–SAM–gold slide electrode without light illumination (Figure S4) or the SAM-only gold slide electrode without CRY1s immobilized (Figures S5 and S6) at different magnetic fields. This is evidence that the changes of oxidation peak current from the CRY1s–SAM–gold slide at different magnetic fields (Figures S7 and S8) result from concurrence of blue light excitation and magnetic field effects on CRY1s (see more in the Methods Section for control experiments).

Association strength and stability of the adsorbed CRY1 films were assessed by voltammograms. This was performed using the same CRY1s–SAM–gold electrode at subsequent times. In this procedure, the electrode was placed in the supporting electrolyte solution, and after 20 s, a voltammogram was initiated with a scan rate of 4 V s^{-1}. Voltammograms were performed at subsequent time points (each measurement with light excitation but in the absence of the magnetic field) until the peak current was found to stabilize. The peak current is proportional to the amount of CRY1 adsorbed on the surface. Thus, Figure 2B shows a profile of the adsorbed species concentration as a function of time. The peak current is found to stabilize after 110 min, and 91.3 ± 0.2% of the initial amount of CRY1 adsorbed on the surface is maintained after 120 min, indicating good stability of immobilized CRY1 at the gold slide surface.

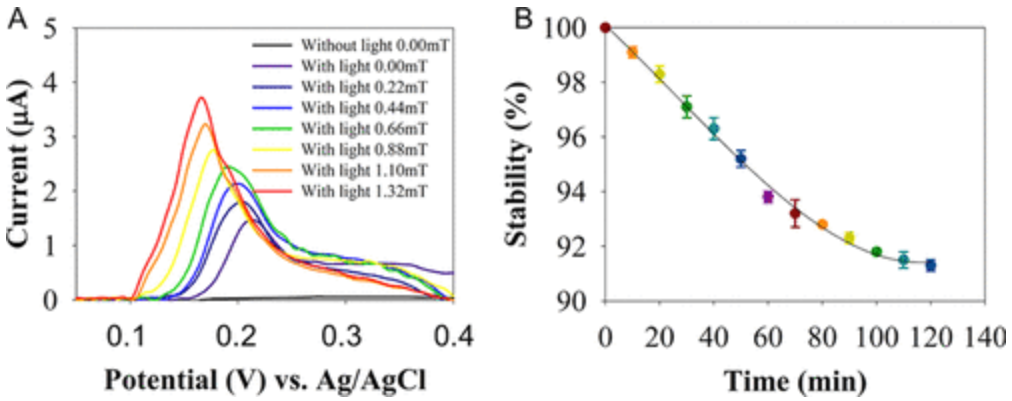

Figure 2.(A) Cyclic voltammograms for the gold slide surface immobilized with CRY1 with and without blue light excitation in the absence of the magnetic field and with blue light excitation under different magnetic fields at the scan rate of 4 V s^{-1}. (B) Time profiles for the surface concentration of immobilized CRY1 with blue light excitation at the scan rate of 4 V s^{-1} in the absence of the magnetic field.

Magnetic Response of Photoactivated CRY1. During cyclic voltammetry, the peak current, i_p, displays as a function of the voltage scan rate, ν, for the stabilized CRY1–SAM–gold electrodes in an external magnetic field. Specifically, the magnitude of the peak current was found to increase linearly with the scan rate, which is consistent with the redox reaction of immobilized species at electrode surfaces.(47) The data in Figure 2A show that the oxidation peak potential shifts to lower values with the increasing magnetic field, and the data in Figure 3A show that the slope of the peak current versus scan rate plot (Table S1) increases more strongly at higher magnetic fields, suggesting that the electron transfer rate increases with the increase of the magnetic field strength.(47)

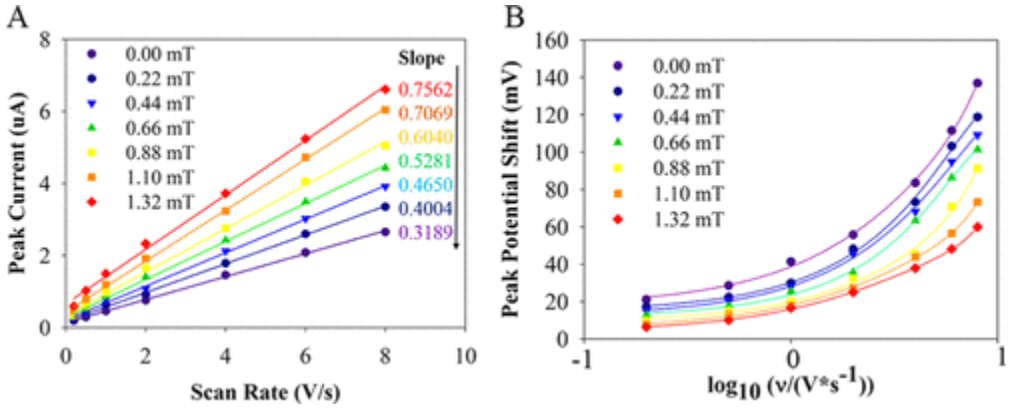

Figure 3. (A) Linear dependence of the peak current on the voltage scan rate under different magnetic fields. (B) Dependence of the peak potential on log(scan rate, ν) under different magnetic fields and fits of the data to the extended Marcus model for electron transfer (at λ = 0.8 eV). Note that the scan rates (ν) are 0.2, 0.5, 1, 2, 4, 6, and 8 V s^{-1}.

The dependence of the oxidation peak's position on the voltage scan rate can be used to extract an electron transfer rate constant.(48−50) The electron transfer between an immobilized, electroactive reporter, such as CRY1, and an electrode can be written as

$$\mathrm{CRY1}^{*} \xrightarrow{k_{ox}} \text{electrode} \tag{1}$$

where the excited CRY1* is the electron donor and the electrode is the electron acceptor during the oxidation reaction. In electrochemistry, the rate constant, k_{ox}, is subject to the overpotential, η. On the basis of the extended Marcus theory for heterogeneous electron transfer,[48−50] the standard heterogeneous rate constant (k^0), that is, the rate constant at η = 0, can be expressed as (see details in the Supporting Information)

$$k^0 = \frac{2\pi}{\hbar}|H_{\mathrm{DA}}|^2 \frac{1}{\sqrt{4\pi\lambda k_{\mathrm{B}}T}} \int_{-\infty}^{\infty} \rho(\varepsilon) f(\varepsilon) \exp\left(-\frac{\left(\lambda + (\varepsilon_{\mathrm{F}} - \varepsilon)\right)^2}{4\lambda k_{\mathrm{B}}T}\right) \mathrm{d}\varepsilon \tag{2}$$

in which, $\hbar$ is the Planck constant, H_{DA} is the effective electronic coupling between the electrode and the CRY1 states, λ is the reorganization energy, k_{B} is Boltzmann's constant, T is temperature in Kelvin, ρ(ε) is the electronic density of states of the electrode, f(ε) is the Fermi function, ε_{F} is the Fermi energy, and ε is the energy of an electronic state in the electrode.

Fitting of the Faradaic peak potential shifts from the formal potential as a function of the scan rate, log(ν), was used to obtain k^0 values for the electron transfer rate constant of the CRY1 immobilized on the gold slide (see details in the Supporting Information). Figure 3B shows a plot of the peak shift versus the voltage scan rate under different magnetic fields (Table S2), along with a best fit of the electron transfer rate constant with a typical reorganization energy of 0.8 eV for FAD proteins.[51] For example, in the absence of an external magnetic field, the standard heterogeneous rate constant for the light-excited CRY1s–SAM–gold slide system is calculated to be 13 s^{-1}. In the presence of an external magnetic field, the standard rate constant increases by approximately 15, 38, 77, 131, 200, and 277% at 0.22, 0.44, 0.66, 0.88, 1.10, and 1.32 mT magnetic field, respectively, compared to the k^0 without a magnetic field (Table 1).

Table 1. Electron Transfer Rate Constant Data

magnetic field (mT)	extended Marcus model (0.3 eV) (s^{-1})	extended Marcus model (0.8 eV) (s^{-1})	Laviron method (s^{-1})
0.00	10 ± 2	13 ± 1	33 ± 2
0.22	13 ± 4	15 ± 3	38 ± 3
0.44	15 ± 4	18 ± 4	45 ± 6
0.66	19 ± 1	23 ± 2	49 ± 5
0.88	25 ± 3	30 ± 4	55 ± 5
1.10	32 ± 3	39 ± 3	63 ± 9
1.32	43 ± 4	49 ± 5	74 ± 7

The electrochemical electron transfer kinetics was also analyzed by using the Laviron formalism based on the classical Butler–Volmer theory as[52]

$$k = (1 - \alpha)\, nF\nu_{\mathrm{i}}/RT \tag{3}$$

where α is the transfer coefficient (0.5), F is the Faraday constant, R is the gas constant, and ν_{i} is the intercept of the linear regions in the plot of peak potential shift versus log(ν) (Figure S9). The electron transfer rate constant values are reported in Table 1, the order of which is well-

consistent with that calculated by the extended Marcus theory under magnetic fields. However, because of the nonlinear correlation of the peak potential versus log(v) over the range of the voltammetric scan rates, the extended Marcus model provides a better fit for the rate constant estimation.

The electrochemical electron transfer mechanism and magnetic responses are discussed in combination with the well-established radical pair mechanism as follows. Homo sapiens CRY1 was reported to confer light-independent biological activity; however, it could be stimulated by light into a flavin-based radical pair.[41] According to the photocycle reaction scheme for CRYs from homogeneous studies,[25,30,32,34,38,53] the CRY1 is first photoexcited from the fully oxidized form of the noncovalently bound FAD cofactor (FAD_{ox}) to produce an excited singlet state ($^1FAD^*$). The $^1FAD^*$ is rapidly reduced by electron transfer along a chain of three Trp residues within the protein to form the radical pair $^1[FAD^{\bullet-}\ TrpH^{\bullet+}]$. The radical pair contains the spin-correlated singlet state of the two unpaired electron spins, one on each radical. The $^1[FAD^{\bullet-}\ TrpH^{\bullet+}]$ radical pair then undergoes either an interconversion of singlet-triplet states between $^1[FAD^{\bullet-}\ TrpH^{\bullet+}]$ and $^3[FAD^{\bullet-}\ TrpH^{\bullet+}]$ (named RP1), which are magnetically sensitive, or a spin-independent (de) protonation of one or both of the radicals (i.e., $FAD^{\bullet-} \rightarrow FADH^{\bullet}$ and/or $TrpH^{\bullet+} \rightarrow Trp^{\bullet}$) to give a long-lived, magnetic-insensitive secondary radical pair in the forms of $[FADH^{\bullet}\ TrpH^{\bullet+}]$, $[FAD^{\bullet-}\ Trp^{\bullet}]$, or $[FADH^{\bullet}\ TrpH^{\bullet}]$ (RP2). Meanwhile, the $^1[FAD^{\bullet-}\ TrpH^{\bullet+}]$ proceeds with spin-allowed reverse electron transfer to regenerate the ground oxidation state (FAD_{ox} + TrpH).[53] The time scale of singlet $^1[FAD^{\bullet-}\ TrpH^{\bullet+}]$ to the ground oxidation state (FAD_{ox} + TrpH) or from RP1 to RP2 is in the μs range, whereas the RP2 has a longer lifetime on the order of milliseconds. The radicals in RP2 then turn back to their respective ground states by two independent slow redox reactions at the time scale of ms (k_F and k_D in Figure 4).[32] The slow radical termination reactions are one of the key steps to lead to a significant amplification of the effects of weak magnetic fields on FAD-containing radical pairs under conditions of continuous photoexcitation.[32,37,54]

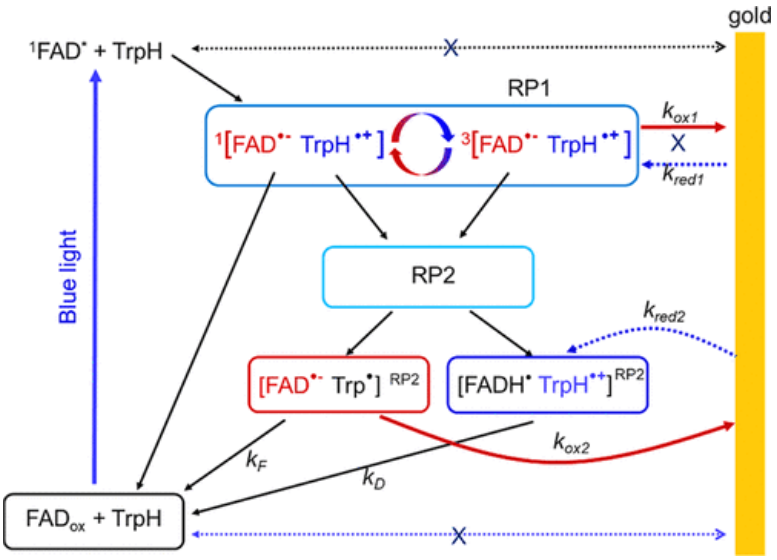

Figure 4. Proposed electrochemical reaction and electron transfer pathways of CRY1 immobilized at the gold electrode based on the photocycle scheme of CRYs and the magnetic sensitive radical pair mechanism.

Assuming that the CRY1 follows the radical pair mechanism of cryptochromes for its magnetic field effect, a hypothesized photoinduced electron reaction diagram at the electrode is proposed and depicted in Figure 4. Because the FAD_{ox} is embedded in the protein and undergoes fast light excitation (femto-picosecond), there is little FAD_{ox} available for the reduction reaction from the ground states of FAD_{ox} by cyclic voltammetry.[55] When the FAD is excited to be FAD*, which is rapidly converted to radical pairs (picosecond),[25,30] the electron transfer between FAD* and the electrode is unlikely to ensue. According to the existing forms of the radical pair, the possible electron transfer reactions between the photoactivated radicals and the electrode are proposed to be

$$[\mathrm{FAD}^{\bullet-}\mathrm{TrpH}^{\bullet+}]^{\mathrm{RP1}} \xrightarrow{k_{\mathrm{ox1}}} \mathrm{FAD_{ox}} + \mathrm{TrpH}^{\bullet+} + \mathrm{e} \tag{4}$$

$$[\mathrm{TAD}^{\bullet-}\mathrm{TrpH}^{\bullet+}]^{\mathrm{RP1}} + \mathrm{e} \xrightarrow{k_{\mathrm{red1}}} \mathrm{FAD}^{\bullet-} + \mathrm{TrpH} \tag{5}$$

$$[\mathrm{FAD}^{\bullet-}\mathrm{Trp}^{\bullet}]^{\mathrm{RP2}} \xrightarrow{k_{\mathrm{ox2}}} \mathrm{FAD_{ox}} + \mathrm{Trp}^{\bullet} + \mathrm{e} \tag{6}$$

$$[\mathrm{FADH}^{\bullet}\mathrm{TrpH}^{\bullet+}]^{\mathrm{RP2}} + \mathrm{e} \xrightarrow{k_{\mathrm{red2}}} \mathrm{FADH}^{\bullet} + \mathrm{TrpH} \tag{7}$$

Because of the short time scale (μs) of relaxation processes from $^1[FAD^{\bullet-}\ TrpH^{\bullet+}]$ to the ground state (FAD_{ox} + TrpH) and the rate of RP1 to RP2,[53] it is unlikely that the process represented by eq 4 or 5 is detectable in the scan rate of the cyclic voltammetry in this study. Hence, eq 6 is probably the electron transfer reaction corresponding to the oxidative Faradaic current in the photoinduced electrochemistry of the immobilized CRY1s because of the slow (∼ms) relaxation reaction of RP2 to the ground state (FAD_{ox} + TrpH). However, it should not be a direct electron transfer from FAD because of the depth of embedment within the protein. This has happened on FAD in glucose oxidase when immobilized through the SAM bridge at a gold electrode.[55] Instead, the oxidative electron transfer could be mediated by the conserved triad of Trp residues[35,38,56−58] or by tunneling through surrounding residues, such as the α-helix (α-15) between residues D358 and the phenyl ring of F366,[31,59] to the gold electrode. This peak is also unlikely to be the oxidation of the ground state of FAD because the potential of direct oxidation of FAD in enzymes is normally at more negative potentials.[51,55,60] The radical cation $TrpH^{\bullet+}$ in RP2 is probably functioning as an acceptor of the electron from the gold electrode (eq 7); however, it is not observed in the cyclic voltammograms. Its reduction potential may lie outside the CV scan voltage window because the reduction potential of free L-Trp is larger than 0.8 V versus Ag/AgCl in cyclic voltammetry.[61]

Sensitivity to Magnetic Field. The electrochemical measurements in this work were operated by maintaining gold slide electrodes in the same orientation at the same position located at center of the Helmholtz coil. Hence, the results should be comparable. The correlation of the Faradaic current and electron transfer rate constant to the external magnetic field is shown in Figure 5. The peak current has a linear dependence on the magnetic field strength (Figures 5A and S10) with an increasing magnitude of the Faradaic current at a higher field strength. Likewise, the ratio of the rate constant increases superlinearly with the magnetic field strength (Figure 5B shows a log plot). For every 50 μT increase (equivalent to earth's magnetic field strength), the calculated rate constant increases 5.7% (Marcus fit).

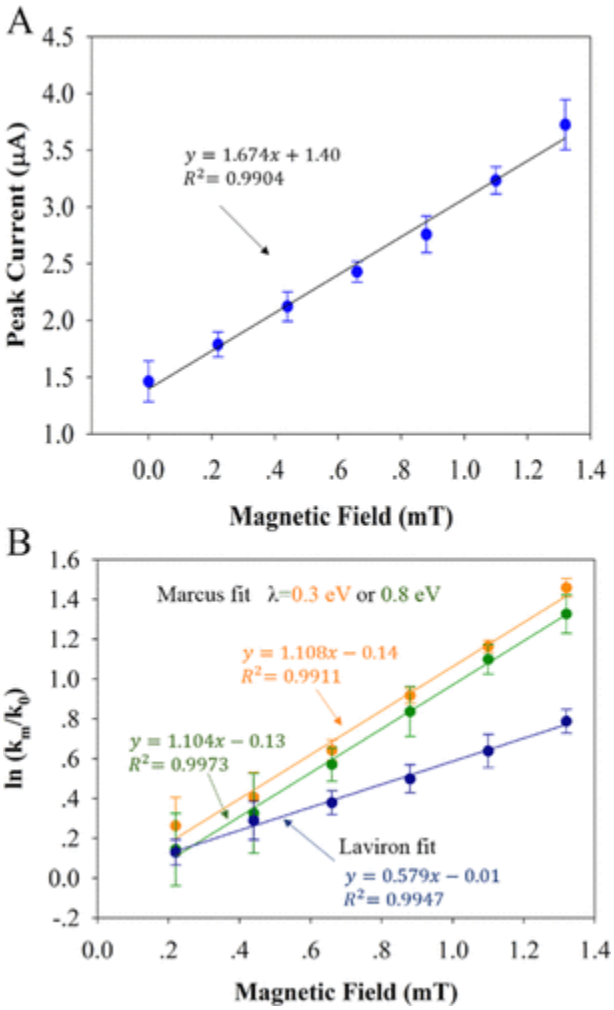

Figure 5. Magnetic sensitivity of (A) peak current (at 4 V s^{-1} scan rate) vs field strength and (B) plot of ln(k_m/k_0) vs field strength for the gold slide surface immobilized with CRY1 under blue light excitation with a linear fit. Note that k_m and k_0 are the calculated rate constant k^0 values in the presence and absence of magnetic fields, respectively.

There is a competition of electron transfer of eq 6 and the k_F of $FAD^{\bullet-}$ to ground-state FAD_{ox}. A spectroscopic study[37] shows that the rate constant of the k_F in Figure 4 has a value of the same order as the electron transfer rate constant reported here, supporting the hypothesis that the reaction eq 6 is electrochemically detectable. A weak external magnetic field (1.32 mT or less) favors the formation of RP2 with a longer life time,[31,53] resulting in more $FAD^{\bullet-}$ involved in the oxidation reaction eq 6. This accounts for the Faradaic current increase with an increased magnetic field.

The next question is why the electron transfer rate constant of the photoactivated CRY1 is sensitive to the weak external magnetic field. The radical pair mechanism predicts that extremely small magnetic interactions can very likely significantly affect the outcome of radical-pair reaction, for example, the RP1 generation and states of the photoactivated CRY1.[25] Though the RP2 state of protein does not actively generate or produce magnetic field effects because the spin

correlation from RP1 should relax before RP2 recombines, the long-lived RP2 protein containing free radical $FAD^{\bullet-}$ inherits the magnetic field effect/information, being stabilized by reduction of $Trp^{\bullet}$ radicals, and is assumed to be responsible for signaling.[25,34] Therefore, the 5.7% change in the rate constant of the free radical $FAD^{\bullet-}$ of RP2 per 50 μT may be associated with the magnetoreception signaling process.

Conclusions

This work demonstrates that external magnetic fields can induce changes in the electron transfer rate from the radicals to the edge of the immobilized CRY1, as well as the magnitude of the electrical signal; it may open a new avenue to studies of the signaling of the photoreceptors and offer promise for the development of a biomimetic optomagneto compass. The significance and the merit of the current work are twofold. This work shows that electrochemistry can be used to investigate the surface-immobilized cryptochromes for magnetic sensing and responses by measuring the heterogeneous electron transfer. The electrode functions as a probe to detect the electrical signal generated from photoactivated cryptochromes under the magnetic field. Scientifically, the results suggest that photoinduced radicals in FAD-bound CRY1 is sensitive to the weak magnetic field, and the long-lived free radical $FAD^{\bullet-}$ is proposed to be responsible for the detected electrochemical Faradaic current because of its oxidation. This is supported by the measured electron transfer constant from the $FAD^{\bullet-}$ in CRY1 which is comparable to the resting rate of the free radical to the ground oxidation state by the homogeneous spectroscopic study. For the photolyase-like photoreceptor, a 5.7% rate constant change in electron transfer reaction corresponding to a 50 μT magnetic field (equivalent to earth magnetic field) may be associated with the protein-signaling process.

Methods

CRY1 Characterization. Ultraviolet–visible spectroscopy (UV–vis spectroscopy, Varian Cary 6000i) over the spectral range of 280–600 nm was used to investigate the absorbance properties of the photolyase-like CRY1 (Novus Biologicals, cat.# NBL1-09495, licensed from OriGene Technologies), and the CRY1 proteins were created in HEK293T cells, using plasmid ID RC207152 and based on accession number NM_004075. The protein contains a C-terminal DDK tag. The gene encodes a FAD-binding protein that is a key component of the circadian core oscillator complex. The proteins extracted with exact buffer (0.125 M Tris, 1% SDS, 10% glycerol, 0.05 M sodium metabisulfite) and purified by amylose affinity chromatography as described previously.[14] The UV–vis measurement was conducted in a solution of 50 mM Tris buffer containing 500 mM NaCl under pH = 8.

Preparation of Immobilized CRY1 onto the Gold Slide Electrode Surface. The gold coated slides contained 20 nm of Au deposited on a 11.5 mm × 11.5 mm glass slide (surface area of 1.32 cm^2) by physical vapor deposition (Kurt Lesker PVD75 E-Beam Evaporator System). Gold slides were first cleaned with O_2 plasma (South Bay Technologies PC2000 Plasma Cleaner) for 3 min. The slides were then incubated in a mixture of 11-mercaptoundecanoic acid ($HS(CH_2)_{10}COOH$, Sigma-Aldrich) and 8-mercapto-octanol ($HS(CH_2)_8OH$, Sigma-Aldrich) in an absolute ethanol solution (ACROS Organics) with a 1:2 mole ratio overnight to form a SAM. After SAM formation, the gold slides were incubated in a 10 mM PBS solution with 0.5 mM 1-

(3-dimethylaminopropyl)-3-ethylcarbodiimide hydrochloride (EDC, TCI)/*N*-hydroxysuccinimide (NHS, Sigma-Aldrich) for 2 h to activate the carboxylic acid groups. Next, the gold slide was rinsed with 10 mM PBS solution and immediately moved to a freshly prepared 10 mM PBS solution containing 1 mg/mL of CRY1 for 2 h in a black box. This was followed by dipping 10 min in a 0.2 M glycine PBS solution to deactivate the remaining active sites on the SAM. The gold slides were rinsed with 10 mM PBS solution and then used for electrochemical measurement.

Electrochemical Measurement. Cyclic voltammetry on immobilized CRY1 was carried out using a Bio-Logic VMP3 electrochemical workstation with a three-electrode testing system. A platinum wire counter electrode (Fisher Scientific), an Ag/AgCl (saturated KCl) reference electrode (Fisher Scientific), and a gold slide that functioned as the working electrode made up the system. Note that the gold slide was in full contact with the electrolyte and was electrically connected through a piece of a copper tape. Cyclic voltammetry measurements were performed in 10 mM PBS at room temperature under a nitrogen environment at the scan rate of 0.2, 0.5, 1, 2, 4, 6, and 8 V s^{-1}. The photoinduced measurement was carried out using a handheld blue laser (447 nm, Big Lasers Co.) with a fully covered illumination area for the gold slide electrode. The temperature of the electrolyte solution was monitored without seeing noticeable changes during the laser illumination and under the magnetic field. Note that experiments were performed with or without an external light and/or magnetic field for a total of four different combinations for each different tested system (SAM/gold slide with/without CRY1 immobilization). Each electrochemical experiment was conducted three times, and the average data are presented.

Magnetic Field Setup. Because the magnetic field of each individual coil is nonuniform, two narrow coils with a large radius, *r* (12.5 cm), were built parallel to one another on the same axis, and with a spacing equal to the radius. The arrangement of the two parallel coils makes the magnetic field uniform in a typical region based on the superimposition of the two fields. An electrochemical cell is placed between the two coils for electrochemical measurements (see Figure 1). Given the Helmholtz arrangement of the pair of coils, the following equation is used to calculate the magnetic field

$$H = 0.72\mu I\frac{N}{r} \tag{8}$$

where H is the magnetic flux density, μ is the magnetic field constant, I is the coil current (in A), N is the number of turns in each coil, and r is the coil radius. After simplifying, using the equation of $H = 0.7433 \times I$ in mT (the unit of I is A), we find the magnetic fields to be 0.22, 0.44, 0.66, 0.88, 1.10, and 1.32 mT by setting the power supply and adjusting the current for the Helmholtz coils. The magnetic fields were also checked by a magnetic field gauss meter (OMEGA).

Control Experiments. A few electrodes were prepared to ensure that the magnetic responsive signal measured in this study is generated from the CRY1 proteins. The control 1 electrode is modified with the mixed SAM of $HS(CH_2)_{10}COOH$ and $HS(CH_2)_8OH$. The control 2 electrode is prepared using the same procedure of protein immobilization, but the incubation solution is the cell lysate solution from an empty vector (no CRY1 in the solution as the negative control of the

purchased CRY1). The control 3 electrode is prepared using the same binding procedure but free FADs are immobilized instead of CRY1. These control electrodes were measured in the cyclic voltammetry upon the blue light illumination under the absence or presence of the magnetic field. No magnetic responses were found from those control electrodes (Figures S5,S6, S11–S14), which ensures that the electrochemical signal changes of CRY1-immobilized electrodes under the magnetic field arise from the photoactivated CRY1 proteins.

Supporting Information

The Supporting Information is available at https://doi.org/10.1021/acsomega.8b00645.

The authors declare no competing financial interest.

Some preliminary results of this work were presented in Zheng's PhD thesis at UNCG library in 2017.

Acknowledgments

This work is partially supported by US NSF (1511194) and NC state funding through the Joint School of Nanoscience and Nanoengineering (JSNN). This work was performed at the Joint School of Nanoscience and Nanoengineering (JSNN), a member of Southeastern Nanotechnology Infrastructure Corridor (SENIC) and National Nanotechnology Coordinated Infrastructure (NNCI), which is supported by the National Science Foundation (ECCS-1542174).

References

1. Gressel, J. Blue light photoreception. *Photochem. Photobiol.* **1979**, *30*, 749– 754, DOI: 10.1111/j.1751-1097.1979.tb07209.x

2. Ahmad, M.; Cashmore, A. R. HY4 gene of A. thaliana encodes a protein with characteristics of a blue-light photoreceptor. *Nature* **1993**, *366*, 162– 166, DOI: 10.1038/366162a0

3. Batschauer, A. A plant gene for photolyase: an enzyme catalyzing the repair of UV-light-induced DNA damage. *Plant J.* **1993**, *4*, 705– 709, DOI: 10.1046/j.1365-313x.1993.04040705.x

4. Lin, C.; Robertson, D.; Ahmad, M.; Raibekas, A.; Jorns, M.; Dutton, P.; Cashmore, A. Association of flavin adenine dinucleotide with the Arabidopsis blue light receptor CRY1. *Science* **1995**, *269*, 968, DOI: 10.1126/science.7638620

5. Hsu, D. S.; Zhao, X.; Zhao, S.; Kazantsev, A.; Wang, R.-P.; Todo, T.; Wei, Y.-F.; Sancar, A. Putative Human Blue-Light Photoreceptors hCRY1 and hCRY2 Are Flavoproteins. *Biochemistry* **1996**, *35*, 13871– 13877, DOI: 10.1021/bi962209o

6. Todo, T.; Ryo, H.; Yamamoto, K.; Toh, H.; Inui, T.; Ayaki, H.; Nomura, T.; Ikenaga, M. Similarity among the Drosophila(6-4) photolyase, a human photolyase homolog, and the

DNA photolyase-blue-light photoreceptor family. *Science* **1996**, *272*, 109, DOI: 10.1126/science.272.5258.109

7. Sancar, A. Structure and Function of DNA Photolyase and Cryptochrome Blue-Light Photoreceptors. *Chem. Rev.* **2003**, *103*, 2203– 2238, DOI: 10.1021/cr0204348

8. Zhao, S.; Sancar, A. Human Blue-light Photoreceptor hCRY2 Specifically Interacts with Protein Serine/Threonine Phosphatase 5 and Modulates Its Activity. *Photochem. Photobiol.* **1997**, *66*, 727– 731, DOI: 10.1111/j.1751-1097.1997.tb03214.x

9. Kobayashi, K.; Kanno, S.-i.; Takao, M.; Yasui, A.; Smit, B.; van der Horst, G. T. J. Characterization of photolyase/blue-light receptor homologs in mouse and human cells. *Nucleic Acids Res.* **1998**, *26*, 5086– 5092, DOI: 10.1093/nar/26.22.5086

10. Miyamoto, Y.; Sancar, A. Vitamin B2-based blue-light photoreceptors in the retinohypothalamic tract as the photoactive pigments for setting the circadian clock in mammals. *Proc. Natl. Acad. Sci. U.S.A.* **1998**, *95*, 6097– 6102, DOI: 10.1073/pnas.95.11.6097

11. Todo, T. Functional diversity of the DNA photolyase/blue light receptor family. *Mutat. Res.* **1999**, *434*, 89– 97, DOI: 10.1016/s0921-8777(99)00013-0

12. Lin, C.; Todo, T. The cryptochromes. *Genome Biol.* **2005**, *6*, 220, DOI: 10.1186/gb-2005-6-5-220

13. Brautigam, C. A.; Smith, B. S.; Ma, Z.; Palnitkar, M.; Tomchick, D. R.; Machius, M.; Deisenhofer, J. Structure of the photolyase-like domain of cryptochrome 1 from Arabidopsis thaliana. *Proc. Natl. Acad. Sci. U.S.A.* **2004**, *101*, 12142– 12147, DOI: 10.1073/pnas.0404851101

14. Malhotra, K.; Kim, S.-T.; Batschauer, A.; Dawut, L.; Sancar, A. Putative blue-light photoreceptors from Arabidopsis thaliana and Sinapis albawith a high degree of sequence homology to DNA photolyase contain the two photolyase cofactors but lack DNA repair activity. *Biochemistry* **1995**, *34*, 6892– 6899, DOI: 10.1021/bi00020a037

15. Chaves, I.; Pokorny, R.; Byrdin, M.; Hoang, N.; Ritz, T.; Brettel, K.; Essen, L.-O.; van der Horst, G. T. J.; Batschauer, A.; Ahmad, M. The Cryptochromes: Blue Light Photoreceptors in Plants and Animals. *Annu. Rev. Plant Biol.* **2011**, *62*, 335– 364, DOI: 10.1146/annurev-arplant-042110-103759

16. Ritz, T.; Adem, S.; Schulten, K. A model for photoreceptor-based magnetoreception in birds. *Biophys. J.* **2000**, *78*, 707– 718, DOI: 10.1016/s0006-3495(00)76629-x

17. Galland, P.; Pazur, A. Magnetoreception in plants. *J. Plant Res.* **2005**, *118*, 371– 389, DOI: 10.1007/s10265-005-0246-y

18. Maffei, M. E. Magnetic field effects on plant growth, development, and evolution. *Front. Plant Sci.* **2014**, *5*, 445, DOI: 10.3389/fpls.2014.00445

19. da Silva, J. A. T.; Dobránszki, J. Magnetic fields: how is plant growth and development impacted?. *Protoplasma* **2016**, *253*, 231– 248, DOI: 10.1007/s00709-015-0820-7

20. Rodgers, C. T.; Hore, P. J. Chemical magnetoreception in birds: The radical pair mechanism. *Proc. Natl. Acad. Sci. U.S.A.* **2009**, *106*, 353– 360, DOI: 10.1073/pnas.0711968106

21. Solov'yov, I. A.; Greiner, W. Micromagnetic insight into a magnetoreceptor in birds: Existence of magnetic field amplifiers in the beak. *Phys. Rev. E: Stat., Nonlinear, Soft Matter Phys.* **2009**, *80*, 041919, DOI: 10.1103/physreve.80.041919

22. Qin, S.; Yin, H.; Yang, C.; Dou, Y.; Liu, Z.; Zhang, P.; Yu, H.; Huang, Y.; Feng, J.; Hao, J.; Hao, J.; Deng, L.; Yan, X.; Dong, X.; Zhao, Z.; Jiang, T.; Wang, H.-W.; Luo, S.-J.; Xie, C. A magnetic protein biocompass. *Nat. Mater.* **2016**, *15*, 217– 226, DOI: 10.1038/nmat4484

23. Ritz, T.; Thalau, P.; Phillips, J. B.; Wiltschko, R.; Wiltschko, W. Resonance effects indicate a radical-pair mechanism for avian magnetic compass. *Nature* **2004**, *429*, 177– 180, DOI: 10.1038/nature02534

24. Dodson, C. A.; Hore, P. J.; Wallace, M. I. A radical sense of direction: signalling and mechanism in cryptochrome magnetoreception. *Trends Biochem. Sci.* **2013**, *38*, 435– 446, DOI: 10.1016/j.tibs.2013.07.002

25. Hore, P. J.; Mouritsen, H. The Radical-Pair Mechanism of Magnetoreception. *Annu. Rev. Biophys.* **2016**, *45*, 299– 344, DOI: 10.1146/annurev-biophys-032116-094545

26. Harris, S.-R.; Henbest, K. B.; Maeda, K.; Pannell, J. R.; Timmel, C. R.; Hore, P. J.; Okamoto, H. Effect of magnetic fields on cryptochrome-dependent responses in Arabidopsis thaliana. *J. R. Soc., Interface* **2009**, *6*, 1193– 1205, DOI: 10.1098/rsif.2008.0519

27. Solov'yov, I. A.; Domratcheva, T.; Moughal Shahi, A. R.; Schulten, K. Decrypting Cryptochrome: Revealing the Molecular Identity of the Photoactivation Reaction. *J. Am. Chem. Soc.* **2012**, *134*, 18046– 18052, DOI: 10.1021/ja3074819

28. Solov'yov, I. A.; Schulten, K. Reaction Kinetics and Mechanism of Magnetic Field Effects in Cryptochrome. *J. Phys. Chem. B* **2012**, *116*, 1089– 1099, DOI: 10.1021/jp209508y

29. Niessner, C.; Denzau, S.; Stapput, K.; Ahmad, M.; Peichl, L.; Wiltschko, W.; Wiltschko, R. Magnetoreception: activated cryptochrome 1a concurs with magnetic orientation in birds. *J. R. Soc., Interface* **2013**, *10*, 20130638, DOI: 10.1098/rsif.2013.0638

30. Kao, Y.-T.; Tan, C.; Song, S.-H.; Öztürk, N.; Li, J.; Wang, L.; Sancar, A.; Zhong, D. Ultrafast Dynamics and Anionic Active States of the Flavin Cofactor in Cryptochrome and Photolyase. *J. Am. Chem. Soc.* **2008**, *130*, 7695– 7701, DOI: 10.1021/ja801152h

31. Henbest, K. B.; Maeda, K.; Hore, P. J.; Joshi, M.; Bacher, A.; Bittl, R.; Weber, S.; Timmel, C. R.; Schleicher, E. Magnetic-field effect on the photoactivation reaction of Escherichia coli DNA photolyase. *Proc. Natl. Acad. Sci. U.S.A.* **2008**, *105*, 14395– 14399, DOI: 10.1073/pnas.0803620105

32. Kattnig, D. R.; Solov'yov, I. A.; Hore, P. J. Electron spin relaxation in cryptochrome-based magnetoreception. *Phys. Chem. Chem. Phys.* **2016**, *18*, 12443– 12456, DOI: 10.1039/c5cp06731f

33. Bialas, C.; Jarocha, L. E.; Henbest, K. B.; Zollitsch, T. M.; Kodali, G.; Timmel, C. R.; Mackenzie, S. R.; Dutton, P. L.; Moser, C. C.; Hore, P. J. Engineering an Artificial Flavoprotein Magnetosensor. *J. Am. Chem. Soc.* **2016**, *138*, 16584– 16587, DOI: 10.1021/jacs.6b09682

34. Sheppard, D. M. W.; Li, J.; Henbest, K. B.; Neil, S. R. T.; Maeda, K.; Storey, J.; Schleicher, E.; Biskup, T.; Rodriguez, R.; Weber, S.; Hore, P. J.; Timmel, C. R.; Mackenzie, S. R. Millitesla magnetic field effects on the photocycle of an animal cryptochrome. *Sci. Rep.* **2017**, *7*, 42228, DOI: 10.1038/srep42228

35. Cailliez, F.; Müller, P.; Firmino, T.; Pernot, P.; de la Lande, A. Energetics of Photoinduced Charge Migration within the Tryptophan Tetrad of an Animal (6–4) Photolyase. *J. Am. Chem. Soc.* **2016**, *138*, 1904– 1915, DOI: 10.1021/jacs.5b10938

36. Hiscock, H. G.; Worster, S.; Kattnig, D. R.; Steers, C.; Jin, Y.; Manolopoulos, D. E.; Mouritsen, H.; Hore, P. J. The quantum needle of the avian magnetic compass. *Proc. Natl. Acad. Sci. U.S.A.* **2016**, *113*, 4634– 4639, DOI: 10.1073/pnas.1600341113

37. Kattnig, D. R.; Evans, E. W.; Déjean, V.; Dodson, C. A.; Wallace, M. I.; Mackenzie, S. R.; Timmel, C. R.; Hore, P. J. Chemical amplification of magnetic field effects relevant to avian magnetoreception. *Nat. Chem.* **2016**, *8*, 384, DOI: 10.1038/nchem.2447

38. Giovani, B.; Byrdin, M.; Ahmad, M.; Brettel, K. Light-induced electron transfer in a cryptochrome blue-light photoreceptor. *Nat. Struct. Mol. Biol.* **2003**, *10*, 489– 490, DOI: 10.1038/nsb933

39. Sancar, A. Regulation of the Mammalian Circadian Clock by Cryptochrome. *J. Biol. Chem.* **2004**, *279*, 34079– 34082, DOI: 10.1074/jbc.r400016200

40. Buhr, E. D.; Takahashi, J. S. Molecular components of the mammalian circadian clock. *Handbook of Experimental Pharmacology*; Springer: 2013, pp 3– 27.

41. Vieira, J.; Jones, A. R.; Danon, A.; Sakuma, M.; Hoang, N.; Robles, D.; Tait, S.; Heyes, D. J.; Picot, M.; Yoshii, T.; Helfrich-Förster, C.; Soubigou, G.; Coppee, J.-Y.; Klarsfeld, A.; Rouyer, F.; Scrutton, N. S.; Ahmad, M. Human Cryptochrome-1 Confers Light Independent Biological Activity in Transgenic Drosophila Correlated with Flavin Radical Stability. *PLoS One* **2012**, *7*, e31867 DOI: 10.1371/journal.pone.0031867

42. Kutta, R. J.; Archipowa, N.; Johannissen, L. O.; Jones, A. R.; Scrutton, N. S. Vertebrate Cryptochromes are Vestigial Flavoproteins. *Sci. Rep.* **2017**, *7*, 44906, DOI: 10.1038/srep44906

43. Sanders, M.; Lin, Y.; Wei, J.; Bono, T.; Lindquist, R. G. An enhanced LSPR fiber-optic nanoprobe for ultrasensitive detection of protein biomarkers. *Biosens. Bioelectron.* **2014**, *61*, 95– 101, DOI: 10.1016/j.bios.2014.05.009

44. Wei, J.; Liu, H.; Khoshtariya, D. E.; Yamamoto, H.; Dick, A.; Waldeck, D. H. Electron-Transfer Dynamics of Cytochrome C: A Change in the Reaction Mechanism with Distance. *Angew. Chem., Int. Ed.* **2002**, *41*, 4700– 4703, DOI: 10.1002/anie.200290021

45. Hill, E.; Ritz, T. Can disordered radical pair systems provide a basis for a magnetic compass in animals?. *J. R. Soc., Interface* **2010**, *7*, S265– S271, DOI: 10.1098/rsif.2009.0378.focus

46. Lau, J. C. S.; Wagner-Rundell, N.; Rodgers, C. T.; Green, N. J. B.; Hore, P. J. Effects of disorder and motion in a radical pair magnetoreceptor. *J. R. Soc., Interface* **2009**, *7*, S257, DOI: 10.1098/rsif.2009.0399.focus

47. Wei, J.; Liu, H.; Dick, A. R.; Yamamoto, H.; He, Y.; Waldeck, D. H. Direct Wiring of Cytochrome c's Heme Unit to an Electrode: Electrochemical Studies. *J. Am. Chem. Soc.* **2002**, *124*, 9591– 9599, DOI: 10.1021/ja025518c

48. Weber, K.; Creager, S. E. Voltammetry of Redox-Active Groups Irreversibly Adsorbed onto Electrodes. Treatment Using the Marcus Relation between Rate and Overpotential. *Anal. Chem.* **1994**, *66*, 3164– 3172, DOI: 10.1021/ac00091a027

49. Khoshtariya, D. E.; Wei, J.; Liu, H.; Yue, H.; Waldeck, D. H. Charge-Transfer Mechanism for Cytochrome c Adsorbed on Nanometer Thick Films. Distinguishing Frictional Control from Conformational Gating. *J. Am. Chem. Soc.* **2003**, *125*, 7704– 7714, DOI: 10.1021/ja034719t

50. Yin, X.; Wierzbinski, E.; Lu, H.; Bezer, S.; de Leon, A. R.; Davis, K. L.; Achim, C.; Waldeck, D. H. A Three-Step Kinetic Model for Electrochemical Charge Transfer in the Hopping Regime. *J. Phys. Chem. A* **2014**, *118*, 7579– 7589, DOI: 10.1021/jp502826e

51. Liu, Y.; Dolidze, T. D.; Singhal, S.; Khoshtariya, D. E.; Wei, J. New Evidence for a Quasi-Simultaneous Proton-Coupled Two-Electron Transfer and Direct Wiring for Glucose Oxidase Captured by the Carbon Nanotube–Polymer Matrix. *J. Phys. Chem. C* **2015**, *119*, 14900– 14910, DOI: 10.1021/acs.jpcc.5b02796

52. Laviron, E. General expression of the linear potential sweep voltammogram in the case of diffusionless electrochemical systems. *J. Electroanal. Chem. Interfacial Electrochem.* **1979**, *101*, 19– 28, DOI: 10.1016/s0022-0728(79)80075-3

53. Maeda, K.; Robinson, A. J.; Henbest, K. B.; Hogben, H. J.; Biskup, T.; Ahmad, M.; Schleicher, E.; Weber, S.; Timmel, C. R.; Hore, P. J. Magnetically sensitive light-induced reactions in cryptochrome are consistent with its proposed role as a magnetoreceptor. *Proc. Natl. Acad. Sci. U.S.A.* **2012**, *109*, 4774– 4779, DOI: 10.1073/pnas.1118959109

54. Evans, E. W.; Kattnig, D. R.; Henbest, K. B.; Hore, P. J.; Mackenzie, S. R.; Timmel, C. R. Sub-millitesla magnetic field effects on the recombination reaction of flavin and ascorbic acid radicals. *J. Chem. Phys.* **2016**, *145*, 085101, DOI: 10.1063/1.4961266

55. Holland, J. T.; Lau, C.; Brozik, S.; Atanassov, P.; Banta, S. Engineering of Glucose Oxidase for Direct Electron Transfer via Site-Specific Gold Nanoparticle Conjugation. *J. Am. Chem. Soc.* **2011**, *133*, 19262– 19265, DOI: 10.1021/ja2071237

56. Biskup, T.; Schleicher, E.; Okafuji, A.; Link, G.; Hitomi, K.; Getzoff, E. D.; Weber, S. Direct Observation of a Photoinduced Radical Pair in a Cryptochrome Blue-Light Photoreceptor. *Angew. Chem., Int. Ed.* **2009**, *48*, 404– 407, DOI: 10.1002/anie.200803102

57. Müller, P.; Yamamoto, J.; Martin, R.; Iwai, S.; Brettel, K. Discovery and functional analysis of a 4th electron-transferring tryptophan conserved exclusively in animal cryptochromes and (6-4) photolyases. *Chem. Commun.* **2015**, *51*, 15502– 15505, DOI: 10.1039/c5cc06276d

58. Zeugner, A.; Byrdin, M.; Bouly, J.-P.; Bakrim, N.; Giovani, B.; Brettel, K.; Ahmad, M. Light-induced Electron Transfer in Arabidopsis Cryptochrome-1 Correlates with in Vivo Function. *J. Biol. Chem.* **2005**, *280*, 19437– 19440, DOI: 10.1074/jbc.c500077200

59. Saxena, C.; Sancar, A.; Zhong, D. Femtosecond Dynamics of DNA Photolyase: Energy Transfer of Antenna Initiation and Electron Transfer of Cofactor Reduction. *J. Phys. Chem. B* **2004**, *108*, 18026– 18033, DOI: 10.1021/jp048376c

60. Thirumalraj, B.; Palanisamy, S.; Chen, S.-M.; Yang, C.-Y.; Periakaruppan, P.; Lou, B.-S. Direct electrochemistry of glucose oxidase and sensing of glucose at a glassy carbon electrode modified with a reduced graphene oxide/fullerene-C60 composite. *RSC Adv.* **2015**, *5*, 77651– 77657, DOI: 10.1039/c5ra12018g

61. Fan, Y.; Liu, J.-H.; Lu, H.-T.; Zhang, Q. Electrochemistry and voltammetric determination of L-tryptophan and L-tyrosine using a glassy carbon electrode modified with a Nafion/TiO_2-graphene composite film. *Microchim. Acta* **2011**, *173*, 241– 247, DOI: 10.1007/s00604-011-0556-9